Organometallics **1996,** *15,* 3844−3849

Periodic Trends and Ligand Effects in Transition Metal Dihydrogen Complexes: A Quasi-relativistic Density Functional Study

Jian Li and Tom Ziegler*

Department of Chemistry, University of Calgary, Calgary, Alberta, Canada T2N 1N4

Received December 13, 1995[⊗]

A nonlocal, quasi-relativistic density functional method has been applied in a study of dihydrogen and dihydride isomers of $M(CO)_3(PH_3)_2H_2$ (M = Cr, Mo, W) and $Mo(CO)_n(PH_3)_{5-n}H_2$ ($n = 1, 3, 5$). The optimized structures and calculated energetics are in good agreement with available experimental data. The H_2 dissociation energies in the dihydrogen complexes $M(CO)_3(PH_3)_2(H_2)$ (M = Cr, Mo, W) exhibit a typical V-like trend along the triad, as in other transition metal carbonyls and π-complexes. An extended transition state energy decomposition scheme revealed that both H_2 to metal donation and metal to H_2 back-donation increase down the triad. The back-donation, as well as the degree of H_2 activation, decreases with the number of strong π-accepting ligands. However, the stability of the dihydrogen complex increases compared to its dihydride isomer with the number of strong π-acceptor ligands.

Introduction

Classical dihydride complexes have been known for a long time. They are often synthesized by oxidative addition of dihydrogen to a metal center. More recently, Kubas[1] has shown that dihydrogen might form an η^2-H_2 complex with the metal center without breaking the hydrogen−hydrogen bond. The bonding in these dihydrogen complexes, also referred to as nonclassical hydrides, is readily understood in terms of the Dewar−Chatt−Duncason model[1] with donation[2] of charge from the occupied σ_{H_2} HOMO to empty d orbitals and back-donation from occupied d orbitals to the $\sigma^*_{H_2}$ LUMO. Theoretical[3] as well as experimental[1,4] studies have shown that the relative stability between classical hydrides and their nonclassical valence tautomers is strongly influenced by the nature of the ancillary ligands and the metal center.

Modern density functional theory (DFT) has been used in a previous study[5] to analyze how the relative stability of the two valence tautomers $M(PH_3)_3(H)_4$ and $M(PH_3)_3(H)_2(\eta^2\text{-}H_2)$ was influenced by changing the metal center within the iron triad. It was possible in this investigation to analyze quantitatively the importance of donation and back-donation for the equilibrium between the two valence tautomers. The analysis demonstrated further that relativistic effects are responsible for the observed shift in preference from the nonclassical isomer $M(PH_3)_3H_2(\eta^2\text{-}H_2)$ in the case of M = Fe, Ru to $M(PH_3)_3(H)_4$ in the case of M = Os.

We extend here our investigation of the $M-H_2$ bond to the so-called Kubas complex $W(CO)_3(PR_3)_2(H_2)$, as well as to its chromium and molybdenum congeners. The emphasis is again on how the degrees of donation and back-donation will influence the relative stability of the classical and nonclassical tautomers within a triad. Consideration will also be given to the role of the ancillary ligands by studying the series $Mo(CO)_n(PR_3)_{5-n}(H_2)$ ($n = 1, 3, 5$). Some of the points examined here have been addressed experimentally by Kubas *et al.*[5]

Computational Method

The Amsterdam Density Functional package (ADF) was used throughout this study.[6] An uncontracted triple-ζ STO basis set was employed for the ns, np, nd, (n + 1)s, and (n + 1)p orbitals of the transition metal atoms. For carbon, oxygen, and phosphorus, double-ζ basis sets were adopted for ns and np orbitals with an augmented d polarization function.[7] The inner shells

---

[⊗] Abstract published in *Advance ACS Abstracts,* August 1, 1996.

(1) (a) Kubas, G. J.; Ryan, R. R.; Swanson, B. J.; Vergamini, P. J.; Wasserman, H. J. *J. Am. Chem. Soc.* **1984**, *106*, 451. (b) Kubas, G. J.; Ryan, R. R.; Wroblewski, D. *J. Am. Chem. Soc.* **1986**, *108*, 1339. (c) Kubas, G. J. *Acc. Chem. Res.* **1988**, *21*, 120. (d) Kubas, G. J. *Comments Inorg. Chem.* **1988**, *7*, 17. (e) Heinekey, D. M.; Oldham, W. J., Jr. *Chem. Rev.* **1993**, *93*, 913.

(2) (a) Dewar, M. J. S. *Bull. Soc. Chim. Fr.* **1951**, *18*, C79. (b) Chatt, J.; Duncanson, L. A. *J. Chem. Soc.* **1953**, 2339.

(3) (a) Morris, J. H.; Jessop, P. G. *Coord. Chem. Rev.* **1992**, *121*, 155. (b) Crabtree, R. H.; Hamilton, D. G. *Adv. Organomet. Chem.* **1988**, *28*, 299. (c) Crabtree, R. H. *Angew. Chem., Int. Ed. Engl.* **1993**, *32*, 789.

(4) (a) Hay, P. J. *Chem. Phys. Lett.* **1984**, *103*, 466. (b) Hay, P. J. *J. Am. Chem. Soc.* **1987**, *109*, 705. (c) Kober, E. M.; Hay, P. J. In *The challenge of d and f elements, theory and computation*; ACS Symposium Series 394; Salahub, D. R., Zerner, M. C., Eds.; American Chemical Society: Washington, DC, 1989. (d) Haynes, G. R.; Martin, R. L.; Hay, P. J. *J. Am. Chem. Soc.* **1992**, *114*, 28. (e) Lin, Z.; Hall, M. B. *Inorg. Chem.* **1991**, *30*, 2569. (f) Lin, Z.; Hall, M. B. *J. Am. Chem. Soc.* **1992**, *114*, 2928. (g) Lin, Z.; Hall, M. B. *J. Am. Chem. Soc.* **1992**, *114*, 6102. (h) Lin, Z.; Hall, M. B. *Inorg. Chem.* **1992**, *31*, 4262. (i) Lin, Z.; Hall, M. B. *Organometallics* **1992**, *11*, 3801. (j) Lin, Z.; Hall, M. B. *Organometallics* **1993**, *12*, 4046. (k) Lin, Z.; Hall, M. B. *J. Am. Chem. Soc.* **1994**, *116*, 4446. (l) Sargent, A. L.; Hall, M. B.; Guest, M. F. *J. Am. Chem. Soc.* **1992**, *114*, 517. (m) Sargent, A. L.; Hall, M. C. *Inorg. Chem.* **1992**, *31*, 317. (n) Maseras, F.; Duran, M.; Lledos, A.; Bertran, J. *J. Am. Chem. Soc.* **1991**, *113*, 2879. (o) Maseras, F.; Koga, N.; Morokuma, K. *J. Am. Chem. Soc.* **1993**, *115*, 8313. (p) Maseras, F.; Li, X.-K.; Koga, N.; Morokuma, K. *J. Am. Chem. Soc.* **1993**, *115*, 10974. (q) Pacchioni, G. *J. Am. Chem. Soc.* **1990**, *112*, 80. (r) Pacchioni, G.; Bagus, P. S. *Rent. Lincei. Sci. Nat.* **1991**, *2*, 3. (s) Craw, J. S.; Backskay, G. B.; Hush, N. S. *J. Am. Chem. Soc.* **1994**, *116*, 5937. (t) Dapprich, S.; Frenking, G. *Angew. Chem., Int. Ed. Engl.* **1995**, *34*, 354. (u) Bickelhaupt, M.; Baerends, E. *J. Inorg. Chem.* **1990**, *29*, 350. (v) Kubas, G. J.; Nelson, J. E.; Bryan, J. C.; Eckert, J.; Wisniewski, L.; Zilm, K. *Inorg. Chem.* **1994**, *33*, 2954.

(5) Li, J.; Dickson, R. E.; Ziegler, T. *J. Am. Chem. Soc.*, in press.

(6) (a) Baerends, E. J.; Ellis, D. E.; Ros, P. *Chem. Phys.* **1973**, *2*, 41. (b) Ravenek, W. In *Algorithms and applications on vector and parallel computes*; te Riele, H. J. J., Dekkar, Th. J., van de Vorst, H. A., Eds.; Elsevier: Amsterdam, 1987.

S0276-7333(95)00956-3 CCC: $12.00

were treated by the frozen-core approximation. For hydrogen atoms on phosphine, the basis was of double-ζ quality with one additional p polarization function. The hydrogen bound to the metal center was treated separately with a triple-ζ 1s basis and one p function added. To fit the molecular density and Coulomb potential accurately in each SCF cycle, a set of auxiliary s, p, d, f, and g STO functions was introduced.[8] The numerical integration scheme was that developed by te Velde *et al*.[9] All molecular and fragment geometries were optimized according to the analytical energy gradient method implemented by Versluis and Ziegler[10] at the local density level (LDA)[11] and by Fan and Ziegler at the nonlocal level (NL-SCF).[12] The nonlocal corrections were based on Becke's function for exchange[13] and Perdew's function for correlation.[14]

The relativistic effects were treated by a quasi-relativistic (QR) method.[15] In this method, the Hamiltonian retains terms up to first order in α^2 (α is the fine structure constant $1/c$, where c is the speed of light), which include the contributions from the mass–velocity, Darwin, and spin–orbit terms.[16] The changes in the density induced by the first-order Hamiltonian are taken into account to all orders of α^2. The QR scheme has been extended to include energy gradients of importance for geometry optimizations.[17] The combined nonlocal and quasi-relativistic approach, NL-SCF+QR, represents the highest level of theory employed in the present study. It has been demonstrated that the NL-SCF+QR scheme is well suited for molecules containing heavy transition metal atoms.[18]

To analyze the interaction between H_2 and the metal fragments in a more detailed way, we employed the extended transition state (ETS)[19] method. If we regard H_2 as a whole ligand, the bond energy between H_2 and the ML_n fragment can be decomposed as

$$-\mathrm{DE}(\mathrm{L}_n\mathrm{M}-\mathrm{H}_2) = E_{\mathrm{steric}} + E_{\mathrm{prep}} + E_{\mathrm{orb}} \qquad (1)$$

Here E_{steric} represents the steric interaction energy between fragments H_2 and ML_n. This term stems from the electrostatic interaction between the two fragments as well as the repulsive Pauli contribution due to the two-orbital–four-electron interaction between occupied orbitals on the two fragments. The term E_{prep} comes from the energy required to relax the structures of the free fragments to the geometries adopted in the molecules. The E_{orb} term originates from the bonding interaction between occupied and virtual orbitals on two fragments. This term can be divided further into contributions from different symmetry representations (Γ_i) of the molecular point group preserved during the formation of L_nM-H_2 from H_2 and ML_n:

$$E_{\mathrm{orb}} = \sum_i E(\Gamma_i) \qquad (2)$$

The symmetry decomposition in eq 2 makes it possible to obtain the separate contributions to the total bond energy from donation and back-donation in those cases where the two bonding modes involve orbitals belonging to different symmetry representations, Γ_i.

Results and Discussion

Optimized Structures for $M(CO)_n(PH_3)_{5-n}H_2$. The first dihydrogen species to be structurally characterized was the Kubas[1a] complex $W(CO)_3(PR_3)_2H_2$. Since then, structural data have been obtained for a number of dihydrogen complexes.[1] With regard to group 6 systems, structures based on X-ray crystallography have been reported for $Cr(CO)_3(P^iPr_3)_2H_2$[5] and $W(CO)_3(P^iPr_3)_2H_2$.[1a] Unfortunately, the position of hydrogen atoms cannot be determined accurately by this technique. More accurate M–H and H–H data have been obtained by low-temperature neutron diffraction studies on $Mo(CO)(dmmp)_2H_2$[20] and $W(CO)_3(P^iPr_3)_2H_2$.[1c] The H–H bond distances in $M-H_2$ complexes can also be estimated[21] from J_{HD} NMR coupling constants. Such estimates are available for a large body of systems.[1e]

The geometries for $M(CO)_3(PH_3)_2H_2$ (M = Cr, Mo, W, **1**) and $M(CO)_n(PH_3)_{5-n}H_2$ (M = Mo, $n = 1$, **2** and $n = 5$, **3**) as well as the separate ML_5 and H_2 fragments have been optimized within the C_{2v} constraint. We have considered both the dihydrogen and dihydride configurations, Figure 1. Tables 1 and 2 summarize the DFT-optimized geometrical parameters. The available experimental data and other calculated values are included in the tables for comparison.

It follows from Tables 1 and 2 that the geometries calculated by DFT generally are in reasonable agreement with experimental data. The ML_5 framework of the H_2-ML_5 complex is well reproduced at the NL-SCF+QR level with deviations up to 0.05 Å for the M–L distances. Some of the discrepancies can be ascribed to the use of PH_3 groups in place of bulky phosphine ligands. It follows from Table 1 that relativity contracts the M–L bonds by up to 0.12 Å for the heavier congener tungsten, in agreement with previous findings.[4]

We are primarily interested in the coordination geometry of the hydrogen atoms attached to the metal center. A comparison of the M–H distances calculated by the NL-SCF+QR scheme with X-ray experimental data for complex **1a** of chromium and tungsten exhibits

---

(7) (a) Snijders, J. G.; Baerends, E. J.; Vernooijs, P. *At. Nucl. Data Tables* **1982**, *26*, 483. (b) Vernooijs, P.; Snijders, J. G.; Baerends, E. J. *Slater type basis functions for the whole periodic system*; Internal report; Free University of Amsterdam: Amsterdam, The Netherlands, 1981.

(8) Krijn, J.; Baerends, E. J. *Fit functions in the HFS-method*; Internal Report (in Dutch); University of Amsterdam: Amsterdam, The Netherlands, 1984.

(9) (a) Boerrigter, P. M.; te Velde, G.; Baerends, E. J. *Int. J. Quant. Chem.* **1988**, *33*, 87. (b) te Velde, G.; Baerends, E. J. *J. Comput. Phys.* **1992**, *99*, 84.

(10) Versluis, L.; Ziegler, T. *J. Chem. Phys.* **1988**, *88*, 322.

(11) Vosko, S. H.; Wilk, L.; Nusair, M. *Can. J. Phys.* **1980**, *58*, 1200.

(12) Fan, L.; Ziegler, T. *J. Chem. Phys.* **1991**, *95*, 7401.

(13) Becke, A. *J. Chem. Phys.* **1986**, *84*, 4524.

(14) Perdew, J. P. *Phys. Rev. B* **1986**, *33*, 8822; erratum **1986**, *34*, 7406.

(15) Ziegler, T.; Tschinke, V.; Baerends, E. J.; Snijders, J. G.; Ravenek, W. *J. Phys. Chem.* **1989**, *93*, 3050.

(16) (a) Snijders, J. G.; Baerends, E. J. *Mol. Phys.* **1978**, *36*, 1789. (b) Snijders, J. G.; Baerends, E. J.; Ros, P. *Mol. Phys.* **1979**, *38*, 1909.

(17) Schreckenbach, G.; Ziegler, T.; Li, J. *Int. J. Quant. Chem.* **1995**, in press.

(18) (a) Li, J.; Schreckenbach, G.; Ziegler, T. *J. Phys. Chem.* **1994**, *98*, 4838. (b) Li, J.; Schreckenbach, G.; Ziegler, T. *J. Am. Chem. Soc.* **1995**, *117*, 486. (c) Li, J.; Schreckenbach, G.; Ziegler, T. *Inorg. Chem.* **1995**, *34*, 3245. (d) Jacobsen, H.; Schreckenbach, G.; Ziegler, T. *J. Phys. Chem.* **1994**, *98*, 11410.

(19) (a) Ziegler, T.; Rauk, A. *Theor. Chim. Acta* **1977**, *46*, 1. (b) Baerends, E. J.; Rozendaal, A. *NATO ASI* **1986**, *C176*, 159. (c) Ziegler, T. *NATO ASI* **1992**, *C378*, 367.

(20) Kubas, G. J.; Burns, C. J.; Eckert, J.; Johnson, S.; Larson, A. C.; Vergamini, P. J.; Unkefer, C. J.; Khalsa, G. R. K.; Jackson, S. A.; Eisenstein, O. *J. Am. Chem. Soc.* **1993**, *115*, 569.

(21) Khalsa, G. R. K.; Kubas, G. J.; Unkefer, C. J.; Van der Sluys, L. S.; Kubat-Martin, K. A. *J. Am. Chem. Soc.* **1990**, *112*, 3855.

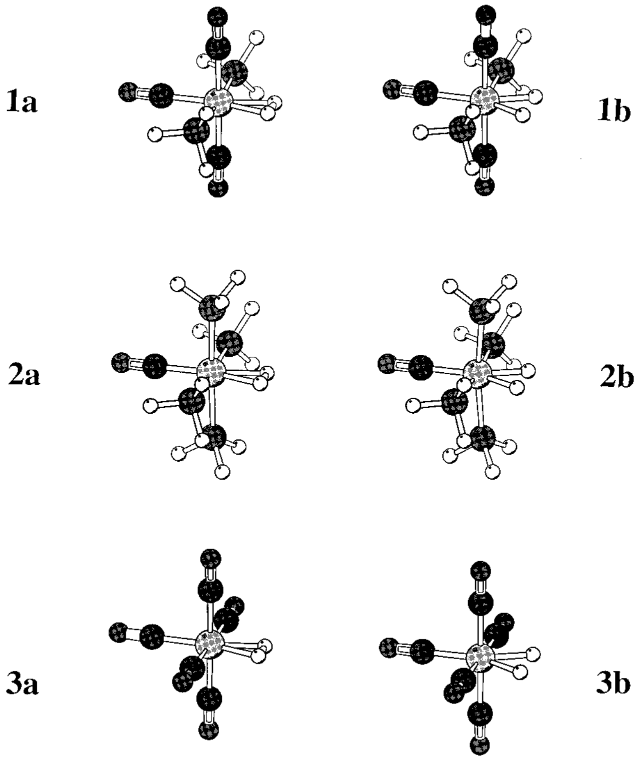

Figure 1. Dihydrogen (**a**) and dihydride (**b**) conformations of $M(CO)_3(PH_3)_2H_2$ (M = Cr, Mo, W) (**1**), $Mo(CO)(PH_3)_4H_2$ (**2**), and $Mo(CO)_4H_2$ (**3**).

a deviation of 0.1 Å. This discrepancy is attributed in part to the difficulties in determining the position of hydrogen atoms near to a heavy metal center by X-ray diffraction. We note in this regard that the H−H distance determined by X-ray is shorter than that of the free H_2 molecule, whereas the calculated H−H distance, as expected, is elongated compared to that of free H_2.

The calculated M−H distances are, on the other hand, consistent with available neutron diffraction data for complex **1a** of tungsten (Table 1) and complex **2a** (Table 2) of molybdenum, with a deviation of about 0.03−0.04 Å. Also, the H−H distances calculated by the NL-SCF+QR method agree within 0.01−0.03 Å with those determined by neutron diffraction, and both sets of data have the H−H distance elongated by 0.10 Å compared to free H_2. The calculated H−H distances are also in good agreement with estimates based on observed J_{HD} coupling constants from NMR spectroscopy.

Other theoretical studies have been carried out on some of the molecules reported in Tables 1 and 2. Hay *et al.*[4b] have optimized the H−H bond distance for $W(CO)_3(PH_3)_2(\eta^2\text{-}H_2)$. Their estimate is in good agreement with experiment and reveals an elongated H−H bond, as in the DFT case. Frenking *et al.*[4t] have optimized the H−H distance for $Mo(CO)5(\eta^2\text{-}H_2)$. The H−H distance of 1.79 Å is 0.03 Å shorter than that found by DFT.

Relative Stability, H_2 Dissociation Energy, and Barrier of Rotation. Relative energies, ΔE, which are defined as the difference in total energy between the dihydride and dihydrogen conformations, are listed in Table 3 for **1** and Table 4 for **2** and **3**. It is clear from the calculated ΔE values that the dihydrogen conformation is the most stable in all cases. This is in agreement with experiment since all structurally characterized $M(CO)_n(PR_3)_{5-n}(H_2)$ complexes with M = Cr, Mo, W and $n = 1, 3, 5$ have a dihydrogen conformation. However, a careful NMR study by Kubas *et al.*[22] indicates that the energy difference between the two conformations is small in the case of $W(CO)_3(P^iPr_3)_2H_2$, with an estimated ΔE value of −1 kcal/mol. Our calculated energy gap is substantially larger, with ΔE given are −10.1 kcal/mol. An even large $-\Delta E$ value, 17 kcal/mol, was obtained by Hay at the Hartree−Fock level for complex **1a** of W.[4b] The MP2 calculation by Lin *et al.* for this molecule gave nearly the same result.[4g] It should be kept in mind that the experimental energy difference is an estimate. Further, PH_3 is likely less electron donating than the P^iPr_3 ligand used in the NMR experiment. Thus, the H−H bond might be further destabilized in the dihydrogen complex $W(CO)_3(P^iPr_3)_2(H_2)$ by back-donation and closer in energy to the dihydride isomer. Relativistic effects are seen to close the energy gap between the two conformers by 0.6 (Cr), 1.9 (Mo), and 3.2 kcal/mol (W). A similar trend has been observed in a previous study.[6]

The H_2 dissociation energy, $DE(L_nM-H_2)$, is calculated as the energy difference between the dihydrogen complex and the fragments $M(CO)_n(PH_3)_{5-n}$ and H_2. Since the zero-point energy is excluded, $DE(L_nM-H_2)$ represents only the electronic contribution to the bond enthalpy. The calculated values are summarized in Tables 3 and 4. Experimentally, the enthalpies for the binding of H_2 to $M(CO)_3(PCy_3)_2$ (M = Cr, Mo, W) have been measured by calorimetric and equilibrium methods.[22] However, these data cannot be directly compared to the absolute L_nM-H_2 bond strength due to the presence of an agostic interaction between the cyclohexyl ring and the metal center at the vacant coordination site in $M(CO)_3(PCy_3)_2$. An estimate of the strength of such an agostic interaction is provided by photoacoustic calorimetry studies of the binding of heptane to $W(CO)_5$. The binding energy was found to be about 13.4 ± 2.8 kcal/mol.[23] Accordingly, the enthalpy of addition of H_2 to the "naked" fragment $W(CO)_3(PCy_3)_2$ is believed to be about −25 kcal/mol.[23] This estimate is close to our calculated $DE(L_nM-H_2)$ value at the NL-SCF+QR level (Tables 3 and 4). By applying the same number for the agostic binding energy to the chromium and molybdenum complexes, the estimated bonding enthalpies are comparable to our calculated $DE(L_nM-H_2)$ values as well. It is important to note that there is a V-like trend for the calculated $DE(L_nM-H_2)$ values within the chromium triad, with molybdenum forming the weakest $M-H_2$ bond. This pattern is in line with the available experimental data. A similar minimum in the $M-H_2$ bond energy at the 4d element was obtained by Frenking *et al.*[4t] in their CCSD(T) study of $M(CO)_5(\eta^2\text{-}H_2)$ (M = Cr, Mo, W), and by Li *et al.*[6] in their investigation of $M(PH_3)_2(H)_2(\eta^2\text{-}H_2)$. *Ab initio* calculations at the HF level for complex **1a** of Mo and W obtained smaller H_2 binding energies[4b] than those reported here. However, the highly correlated CCSD(T) calculation on $Mo(CO)_5(H_2)$ gave $DE(L_nM-H_2)$ = 16.1 kcal/mol,[4t] in good agreement with our NL-SCF+QR result.

---

(22) Gonzalez, A. A.; Zhang, K.; Mukerjee, S. L.; Hoff, C. D.; Khalsa, G. R.; Kubas, G. J. In *Bonding energetics in organometallic compounds*; ACS Symposium Series 428; Marks, T. J., Ed.; American Chemical Society: Washington, DC, 1990.

(23) Morse, J. M.; Parker, G. H.; Burkey, T. J. *Organometallics* **1989**, *8*, 2471.

Table 1. Comparison between Calculated and Observed Geometries for $M(CO)_3(PR_3)_2H_2$[a]

	dihydrogen complexes										dihydride complexes		
	Cr		Mo				W				Cr	Mo	W
parameter	cal(R)	exp[c]	cal(NR)	cal(R)	cal[d]	exp[e]	cal(NR)	cal(R)	cal[d]	exp[f]	cal(R)	cal(R)	cal(R)
$M-C_t$[b]	1.860	1.815	2.023	2.002			2.067	2.013		1.977	1.903	2.076	2.029
$M-C_c$[b]	1.906	1.872	2.070	2.051			2.118	2.033		2.031	1.894	2.054	2.047
M−P	2.324	2.373	2.467	2.455			2.524	2.445		2.495	2.296	2.458	2.360
C_cMC_t[b]	90.0	86.6	90.8	91.1			90.0	89.0		91.9	95.2	94.3	92.5
PMC_t[b]	90.4	93.9	90.4	89.4			90.3	89.2		90.1	88.7	87.4	87.3
M−H	1.857	1.75	1.899	1.897	1.990		1.884	1.872	1.932	1.94(x) 1.89(n)	1.629	1.856	1.817
H−H	0.822	0.67(x)	0.836	0.848	0.784		0.827	0.862	0.806	0.75(x) 0.82(n)	1.438	1.535	1.554
		0.85 (NMR)				0.87 (NMR)				0.89 (NMR)			

[a] Bond lengths in angstroms and bond angles in degrees. cal(NR) and cal(R) correspond to calculated values obtained at the nonrelativistic (NL-SCF) and relativistic levels (NL-SCF+QR), respectively. We indicate X-ray data by (x) and neutron diffraction data by (n). [b] C_t and C_c are the carbon atoms trans and cis to H_2, respectively. [c] X-ray and NMR data from ref 5. [d] *Ab initio* calculation at the HF level.[4b] [e] Reference 5. [f] Reference 1a,e.

Table 2. Geometries of $Mo(CO)_n(PR_3)_{5-n}H_2$ ($n = 1, 3, 5$)[a]

	dihydrogen complexes						dihydride complexes		
	$n = 1$		$n = 3$		$n = 5$		$n = 1$	$n = 3$	$n = 5$
parameter	cal(R)	exp[c]	cal(R)	exp[d]	cal(R)	cal[e]	cal(R)	cal(R)	cal(R)
$M-C_t$[b]	1.984	1.946	2.002		2.021	1.989	2.044	2.076	2.084
$M-C_c$[b]			2.051		2.063 2.066	2.056 2.057		2.054	2.072 2.082
M−P	2.433 2.430	2.423 2.447	2.455				2.426 2.428	2.458	
C_cMC_t[b]			91.1		90.6 89.7	89.0 87.2		94.3	94.4 87.2
PMC_t[b]	91.1 89.2	85.6 98.0	89.4				94.0 87.6	87.2	
M−H	1.896	1.922	1.897		1.899	1.959	1.759	1.856	1.855
H−H	0.855	0.736(n) 0.80−0.85 (n) 0.88 (NMR)	0.848	0.87 (NMR)	0.824	0.791	1.397	1.535	1.516

[a] Bond lengths in angstroms and bond angles in degrees. cal(R) corresponds to calculated values obtained at the relativistic level (NL-SCF+QR). We indicate X-ray data by (x) and neutron diffraction data by (n). [b] C_t and C_c are the carbon atoms trans and cis to H_2, respectively. [c] Reference 21. [d] Reference 5. [e] *Ab initio* calculation at MP2 level.[4t]

Table 3. Relative Energies,[f] H_2 Dissociation Energies, and Rotational Barrier of $M(CO)_3(PH_3)_2H_2$[a]

	ΔE[f]			$DE(L_nM-H_2)$			rotational barrier		
$M(CO)_3(PH_3)_2H_2$	cal(NR)	cal(R)	ab initio	cal(NR)	cal(R)	exp[d]	cal(NR)	cal(R)	exp[e]
$Cr(CO)_3(PH_3)H_2$	−13.2	−12.6		20.8	21.3	7.3 ± 0.1 (23)	1.0	1.2	1.17
$Mo(CO)_3(PH_3)_2H_2$	−11.3	−9.4		17.4	19.2	6.5 ± 0.2 (22)	3.0	3.2	1.32
$W(CO)_3(PH_3)_2H_2$	−13.3	−10.1	−16.7[b] −17.0[c]	17.2	20.9	9.4 ± 1.0 (25)	3.0	3.6	1.9

[a] Energies in kilocalories/mole. cal(NR) and cal(R) correspond to calculated values obtained at the nonrelativistic (NL-SCF) and relativistic levels (NL-SCF+QR), respectively. [b] *Ab initio* calculations at the HF level.[4b] [c] *Ab initio* calculations at the MP2 level.[4g] [d] Bond enthalpies.[23] The data in parentheses are estimated values; see text. [e] Reference 5. [f] The relative energy ΔE is defined as $\Delta E = E$(dihydrogen complex) − E(dihydride complex).

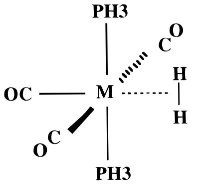

4

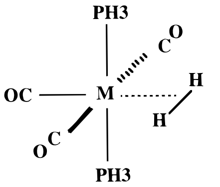

5

The rotational barrier corresponds to the energy difference between **4** and **5**. Here **4** has the H_2 bond vector aligned along the P−M−P axis, whereas the alignment is along the C−M−C axis in **5**. In the NL-SCF and NL-SCF+QR calculations, geometries for both **4** and **5** were fully optimized. Even so, the calculated barrier heights appear to be uniformly larger than those determined by solid state NMR and inelastic neutron scattering spectroscopies,[5,24] especially for complexes of Mo and W. Again, the experimental trend within the triad is reproduced by calculation. Lower barrier heights were obtained by *ab initio* calculation at the HF level,

Table 4. Relative Energies and H_2 Dissociation Energies of $Mo(CO)_n(PH_3)_{5-n}H_2$[a]

	ΔE[c]		DE(LnM−H2)		
	cal(NR)	cal(R)	cal(NR)	cal(R)	*ab initio*
$Mo(CO)(PH_3)_4H_2$	−9.5	−7.9	16.6	18.9	
$Mo(CO)_3(PH_3)_2H_2$	−11.3	−9.6	17.4	19.2	
$Mo(CO)_5H_2$	−18.5	−15.9	18.0	19.6	16.1[b]

[a] Energies in kilocalories/mole. cal(NR) and cal(R) correspond to calculated values obtained at the nonrelativistic (NL-SCF) and relativistic levels (NL-SCF+QR), respectively. [b] *Ab initio* calculation at the CCSD(T) level.[4t] [c] The relative energy ΔE is defined as $\Delta E = E$(dihydrogen complex) − E(dihydride complex).

---

(24) Eckert, J.; Kubas, G. J.; Hall, J. H.; Hay, P. J.; Boyle, C. M. *J. Am. Chem. Soc.* **1990**, *112*, 2324.

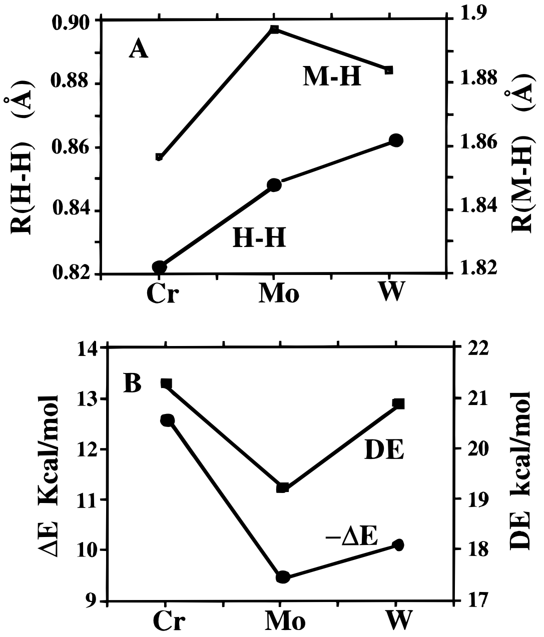

Figure 2. Bond lengths (Å), relative energies, and H_2 dissociation energies (kcal/mol) of $M(CO)_3(PH_3)_2H_2$.

although most of the geometry parameters for **4** and **5** were fixed.[25]

Periodic Trends in $M(CO)_3(PH_3)_2(H_2)$ ($M = Cr$, Mo, W). Some interesting periodic trends can be observed in the calculated properties for complex **1a** of the Cr triad (see Figure 2). If we focus on the geometry parameters relevant to $M-H_2$, it can be seen from Table 1 and Figure 2A that the H−H distances increase down the triad. The same trend has been reported for the NMR-estimated H−H distances. The calculated M−H lengths show a maximum at Mo, which is consistent with the trend existing in M−CO bond lengths for $M(CO)_6$ with M = Cr, Mo, W.[19] The same trend for the M−H bond length has also been reported in geometries of $M(CO)_5(H_2)$ (M = Cr, Mo, W), as optimized at the *ab initio* MP2 level[4t] with relativistic effective core potentials. On the experimental side, it is known that the symmetric and asymmetric $M-H_2$ stretching frequencies for $Mo(CO)_3(PCy_3)_2(H_2)$ (885 and 1420 cm^{-1}) are significantly lower than those for the chromium (950 and 1540 cm^{-1}) and tungsten (951 and 1568 cm^{-1}) congeners. This observation is in harmony with the trend in our calculated M−H bond lengths.

Both the relative energy ΔE and the H_2 dissociation energy $DE(L_nM-H_2)$ of Table 3 display a V-like trend with a minimum at the molybdenum complex (Figure 2B). This is typical for metal−ligand bond strength in complexes where the Dewar−Chatt−Duncanson bonding model is valid. Relativistic effects strengthen the $M-H_2$ bond by 3.7 kcal/mol for the tungsten complex, resulting in an inversion of the ordering of $DE(L_nM-H_2)$ between the tungsten and molybdenum systems. The V-like behavior is also evident in the experimental bond enthalpies for the $M(CO)_3(PCy_3)_2(H_2)$ complexes with M = Cr, Mo, W. For the related $M(CO)_5(H_2)$ complexes of the chromium triad, Frenking *et al.*[4t] also found a V-shaped trend in $DE(L_nM-H_2)$ from their high-level CCSD(T) calculations.

The calculated rotational barrier heights in Table 3 increase down the triad, in parallel with the experimental measurements, although the theoretical values seem to be overestimated in absolute terms. The existence of a rotational barrier has been taken as the most direct proof for the presence of d_π to $\sigma^*_{H_2}$ back-donation. On the basis of the experimentally determined barrier heights, Kubas *et al.* concluded that the back-donation increases down the triad.[5]

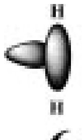

6

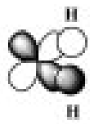

7

By applying the ETS energy decomposition scheme, the relative importance of donation and back-donation for the $M-H_2$ bond strength can be quantified in a more direct way. Table 5 collects the energy components defined in eqs 1 and 2. Since the point group preserved during the formation of complexes **1**−**3** is C_{2v}, the energy contribution from the a_1 representation, $E(a_1)$, accounts for the donation from σ_{H_2} to the metal center (**6**), whereas the contribution from the b_2 representation is attributed to the d_π to $\sigma^*_{H_2}$ back-donation (**7**). It is remarkable that, for complexes **1a**, $E(b_2)$ is slightly larger than $E(a_1)$ in all three molecules, which indicates that the back-donation contribution is comparable to or even larger than the contribution from donation. Both donation and back-donation interactions increase down the triad. It is not difficult to understand this trend since d orbitals become more diffuse down the triad, resulting in more effective bonding overlaps. Relativistic effects are seen to enhance this trend further by increasing the back-donation substantially for the tungsten complex. The underlying reason for this enhancement is the relativistic destabilization of d orbitals.[25] The destabilization decreases the energy gap between $\sigma^*_{H_2}$ and d_π, thus facilitating more back-donation. The relativistic destabilization of the d orbitals is also responsible for enhancing back-donation in transition metal carbonyls and olefin π-complexes.[19] The tendency in our calculated $-E(b_2)$ values is in accordance with the conclusion for the trend in back-donation drawn by Kubas *et al.* from measurements of the rotational barriers.[5]

Ligand Effects in $Mo(CO)_n(PH_3)_{5-n}(H_2)$ ($n = 1, 3, 5$). Most nonclassical dihydrogen complexes of the chromium triad contain carbonyl as well as phosphine ligands. Substitution of a relatively poor π-acceptor such as phosphine by the strongly π-accepting CO ligand has a substantial and predictable impact on the H−H bond length (Table 2) and on the relative energy between the classical and nonclassical hydrides (Table 4). The influence on the $M-H_2$ dissociation energy $DE(L_nM-H_2)$ is more subtle, but follows the expected trend.

Increasing the number of π-accepting carbonyls will diminish the amount of electron density available for back-donation from the metal center to $\sigma^*_{H_2}$. As a consequence, the optimized H−H distances are seen to decrease gradually with n through the series $Mo(CO)_n(PH_3)_{5-n}(H_2)$, $n = 1-5$ (Table 2). This is in harmony with the trend in the experimental H−H stretching frequencies found at 2650, 2950, and 3080 cm^{-1}, re-

---

(25) (a) Pyykkö, P.; Declaux, J.-P. *Acc. Chem. Res.* **1979**, *12*, 276. (b) Schwarz, W. H. E.; van Wezenbeek, E. M.; Baerends, E. J.; Snijders, J. G. *J. Phys. B* **1989**, *22*, 1515.

Table 5. ETS Decomposition of the H_2 Dissociation Energy DE(L_nM-H_2)[a]

	E_{steric}	$-E(a_1)$	$-E(a_2)$	$-E(b_1)$	$-E(b_2)$	$-E_{orb}$	E_{prep}	DE
$Cr(CO)_3(PH_3)_2H_2$	12.0	16.9	0.1	1.2	17.9	36.1	2.8	21.3
$Mo(CO)_3(PH_3)_2H_2$	13.0	17.6	0.0	1.0	18.9	37.5	5.3	19.2
$W(CO)_3(PH_3)_2H_2$ (NR)	13.3	17.1	0.0	1.0	14.8	33.6	3.1	17.2
$W(CO)_3(PH_3)_2H_2$ (R)	11.7	18.2	0.6	0.2	19.5	38.5	5.9	20.9
$Mo(CO)(PH_3)_4H_2$	12.5	13.2	0.2	0.8	21.2	35.4	4.0	18.9
$Mo(CO)_3(PH_3)_2H_2$	13.0	17.6	0.0	1.0	18.9	37.5	5.3	19.2
$Mo(CO)_5H_2$	13.5	23.9	0.4	1.6	11.9	37.8	5.7	19.6

[a] Energies in kilocalories/mole.

spectively for Mo(CO)(dppe)(H_2), $Mo(CO)_3(PCy_3)_2(H_2)$, and $Mo(CO)_5(H_2)$.[5] The stability of the dihydrogen complex relative to the dihydride isomer, $-\Delta E$, increases as more phosphines are substituted by CO from $-\Delta E = 7.9$ kcal/mol for $n = 1$ to $-\Delta E = 9.6$ kcal/mol for $n = 3$ and $-\Delta E = 15.9$ kcal/mol for $n = 5$ (Table 4). The bond strength DE(L_nM-H_2) increases only slightly with n, from 18.9 kcal/mol in $Mo(CO)(PH_3)_4(H_2)$ to 19.6 kcal/mol in $Mn(CO)_5(H_2)$. Lin *et al.* calculated the relative energy, ΔE, for the series $W(CO)_n(PH_3)_{5-n}H_2$ ($n = 0$, 1, 2, 3). They concluded, as expected, that the nonclassical isomers are more likely to be found in complexes with a larger number of π-accepting ligands.[4g]

Our energy decomposition scheme allows us to study in more quantitative detail how the donor−acceptor interactions between the metal center and H_2 are influenced by the nature of the coligands. Such an analysis is shown for the series $Mo(CO)_n(PH_3)_{5-n}(H_2)$ with $n = 1$, 3, 5 in Table 5.

The contribution to DE(L_nM-H_2) from the metal to $\sigma^*_{H_2}$ back-donation $-E(b_2)$, is seen to decrease sharply from 21.2 kcal/mol in $Mo(CO)(PH_3)_4(H_2)$ to 11.9 kcal/mol in $Mo(CO)_5(H_2)$ as the metal center becomes electron poor with the addition of more CO ligands. The donation contribution, $-E(a_1)$, on the other hand, increases with the number of carbonyls as the metal center becomes electron poor. The opposing trends in $-E(a_1)$ and $-E(b_2)$ largely cancel, so that the DE(L_nM-H_2) values for the series are nearly equal.

The two processes represented by $-E(a_1)$ and $-E(b_2)$ involve a weakening of the H−H bond as well as M−H bond formation. As far as H−H bond destabilization is concerned, it is readily shown from simple Huckel considerations that the occupation of $\sigma^*_{H_2}$ will weaken the H−H bond by more than depopulation of σ_{H_2} by the same amount. It is also evident from Tables 2 and 5 that the H−H distance increases with $-E(b_2)$. Thus, back-donation is responsible for H−H activation.

Concluding Remarks

The nonclassical Kubas dihydrogen complex and its congeners have been calculated to be more stable than the classical dihydride isomers by density functional theory at the NL-SCF+QR level. The calculated $M-H_2$ coordination geometries and bond energies compare well with available experimental measurements and estimates. The H_2 bond dissociation energies of $M(CO)_3(PH_3)_2(H_2)$ (M = Cr, Mo, W) show a V-like trend with a minimum at Mo. Together with our previous calculations on metal−ligand bond energies,[19] we can conclude that such V-like trends in bond energies are common and typical in transition metal complexes where the metal−ligand bonding is described by the Dewar−Chatt−Duncanson model. The underlying reason for the V-like behavior is the importance of relativistic effects, especially the relativistic destabilzation of 5d orbitals of third row transition metals.

The influence on the $M-H_2$ bond due to changes in the metal and the ancillary ligands has been explored with the aid of ETS decomposition techniques. Both H_2 to metal donation and metal to H_2 back-donation seem to increase down the triad, which is in part consistent with the conclusions reached by Kubas[5] *et al.*[5] on the basis of observed barriers to rotation for the η^2-H_2 ligand. The back-donation, as well as the degree of activation of H_2, increases as the number of strongly π-accepting ligands such as CO is reduced. On the other hand, the stability of the dihydrogen complex relative to the dihydride isomer increases with the number of strong π-acceptor ligands.

Summary

Density functional theory has been applied to dihydrogen and dihydride isomers of $M(CO)_3(PH_3)_2H_2$ (M = Cr, Mo, W), and $Mo(CO)_n(PH_3)_{5-n}H_2$ ($n = 1$, 3, 5). The H_2 dissociation energies (DE) and M−H distances exhibit a typical V-like trend along the triad due to relativistic effects, as in transition metal carbonyls and π-complexes.

Acknowledgment. This investigation was supported by the Natural Sciences and Engineering Research Council of Canada (NSERC) as well as by the donors of the Petroleum Research Fund, administered by the American Chemical Society. The Academic Computing Services of the University of Calgary is acknowledged for access to the IBM-6000/RISC facilities.

OM950956W